AMSE JOURNALS-2016-Series: Modelling B; Vol. 85; N° 1; pp 43-62
Submitted Feb. 2016; Revised April 16, 2016, Accepted July 15, 2016

Thermal Radiation Effect on MHD 3D Flow and Heat Transfer of Nanofluid past a Shrinking Surface

M. K. Nayak

Department of Physics, Radhakrishna Institute of Technology and Engineering, Bhubaneswar, India.
E-mail: mkn2122@gmail.com

Abstract

In this paper we endeavor to explore the influence of thermal radiation on MHD 3D flow of a nanofluid over a linear shrinking sheet through a porous medium. With the help of similarity transformations, the governing non-linear partial differential equations have been converted into non-linear ordinary differential equations. The series solution of these reduced equations is obtained by using Homotopy Analysis Method (HAM). The non-dimensional velocity and temperature distributions have been presented graphically for various emerging parameters in connection with the problem. It is seen that increase in thermal radiation parameter enhances the fluid temperature and there by the associated thermal boundary layer thickness gets enlarged. Also the skin friction coefficient and Nusselt number for different pertinent parameters are depicted in tabular form.

Keywords: MHD, 3D flow, Shrinking sheet, Thermal radiation. Porous medium.

1. Introduction

By virtue of enormous applications in industries and engineering processes like polymer processing, manufacturing of plastics and metals, research on boundary layer behavior of fluid flow over a continuously shrinking surface keeps going on [1-2]. The pioneer studies in this area were first performed theoretically in [3] and later experimentally by [4]. Further these works were pursued in the analysis [5-8].

A nanofluid is a fluid possessing nanometer sized particles (1-100 nm diameters), called nanoparticles. The concept of nanofluid, has been advanced by Choi [9] through an innovative technique that uses a mixture of solid nanoparticles (Au, Ag, Cu metals, CuO, TiO_2 and Al_2O_3) having higher thermal conductivity and the base fluids (conventional liquids like water, engine oil, toluene, ethylene glycol etc.) of lower thermal conductivity so as to develop advanced heat

transfer fluids with substantial augmentation of thermal conductivities. In other words, highest feasible thermo-physical properties at the smallest feasible concentrations can be accomplished by uniform dispersion and stable suspension of nanoparticles in base fluids. Xuan and Li [10] implemented pure copper particles in the study of convective heat transfer and flow features of nanofluids. They found in their study that the volume fraction, the particle dimensions and material properties play significant role to achieve a substantial augmentation of heat transfer and viscosity.

Nanofluids are widely used in coolants for computers and nuclear reactors, cancer therapy, safer surgery by cooling, lubricants, heat exchangers, micro-channel heat sinks, cooling of a new class of super powerful and small computers and other electronic devices for use in military systems, vehicle cooling and transformer cooling, in designing the waste heat removal equipment, major process industries including materials and chemicals, oil and gas, food and drink, paper and printing etc. as studied in [11].

Recently, Hayat et al. [12] discussed the influence of magnetic field in a three dimensional flow of a nanofluid over a shrinking sheet in presence of convective conditions. However, the authors have not explored the effect of thermal radiation on a nanofluid over a shrinking sheet, which is discussed in the present study.

The thermal radiation effects are of vital importance at high absolute temperature due to basic difference between radiation and convection and conduction energy-exchange mechanisms. For space applications, some devices are designed to operate at high temperature levels in order to obtain high thermal efficiency. That is why the radiation effects are significant while determining thermal effects in the processes with high temperatures. Akber et al. [13] investigated the effect of thermal radiation on MHD convective flow of nanofluid past a shrinking surface. Further, the radiation effects are studied in [14-16].

In this paper, Homotopy analysis method is employed to study the effects of nanoparticle volume fraction (ϕ), magnetic parameter (M), permeability parameter (K_p), shrinking parameter (A), wall mass transfer parameter (f_w), Prandtl number (P_r), radiation parameter (R) on velocity and temperature fields for nanofluids using the thermo physical properties of the base fluid (pure water) and different nanoparticles (kindly see Table 1). To the best of knowledge of the author, yet no attempt has been made to reveal the MHD 3D flow of nanofluid past a shrinking surface with thermal radiation effect.

Nomenclature

(u,v,w)	velocity components along (x, y, z) directions		
υ_{nf}	kinematic viscosity of nanofluid	q_r	radiative heat flux
σ	electrical conductivity	B_0	strength of uniform magnetic field
ρ_{nf}	density of nanofluid	K_p^*	dimensional permeability parameter
α_{nf}	thermal diffusivity of nanofluid	$\left(\rho c_p\right)_{nf}$	heat capacitance of nanofluid
W	wall mass transfer velocity	C_f	skin friction coefficient
a,c,m	constants	σ^*	Boltzmann constant
h	heat transfer coefficient	T	temperature
T_f	temperature of fluid	T_∞	free stream temperature
ϕ	nanoparticle volume fraction	ρ_f	density of the fluid
ρ_s	density of the solid	μ_{nf}	dynamic viscosity of nanofluid
μ_f	dynamic viscosity of fluid	k_{nf}	thermal conductivity of nanofluid
$\left(\rho C_p\right)_f$	heat capacitance of fluid	$\left(\rho C_p\right)_s$	heat capacitance of solid
k_s	thermal conductivity of solid	f	non-dimensional stream function
f'	non-dimensional velocity	η	similarity variable
k_1	mean absorption coefficient	A	shrinking parameter
M	magnetic parameter	K_p	non-dimensional permeability parameter
P_r	Prandtl number	k_f	thermal conductivity of fluid
R	radiation parameter	f_w	wall mass transfer parameter
B_i	Biot's number	Re_x	local Reynolds number
Nu_x	local Nusselt number		

Subscripts

nf	nanofluid
f	fluid
s	solid

Greek Symbols

$\alpha_{nf}, \alpha_f, \phi, \eta$

The objective of the present study is an extension work of Hayat et al. [12]. In the present study, the author has investigated the effect of thermal radiation on the MHD flow and heat transfer of a nanofluid past a permeable shrinking surface through a porous medium by considering nanofluid model-I proposed by Mahdy [17].

2. Formulation of the problem

Consider a steady three dimensional electrical conducting nanofluid over a shrinking surface. Assume that a uniform transverse magnetic field of strength B_0 is imposed parallel to the *z*-axis. Also the induced magnetic and electric fields are assumed to be neglected. The convective boundary conditions are implemented in the heat transfer process. The governing equations are

$$\frac{\partial u}{\partial x}+\frac{\partial v}{\partial y}+\frac{\partial w}{\partial z}=0 \tag{1}$$

$$u\frac{\partial u}{\partial x}+v\frac{\partial u}{\partial y}+w\frac{\partial u}{\partial z}=\upsilon_{nf}\frac{\partial^2 u}{\partial z^2}-\frac{\sigma B_0^2 u}{\rho_{nf}}-\frac{\mu_{nf}}{\rho_{nf}}\frac{u}{K_p^*} \tag{2}$$

$$u\frac{\partial v}{\partial x}+v\frac{\partial v}{\partial y}+w\frac{\partial v}{\partial z}=\upsilon_{nf}\frac{\partial^2 v}{\partial z^2}-\frac{\sigma B_0^2 v}{\rho_{nf}}-\frac{\mu_{nf}}{\rho_{nf}}\frac{v}{K_p^*} \tag{3}$$

$$u\frac{\partial T}{\partial x}+v\frac{\partial T}{\partial y}+w\frac{\partial T}{\partial z}=\alpha_{nf}\frac{\partial^2 T}{\partial z^2}-\frac{1}{\left(\rho C_p\right)_{nf}}\frac{\partial q_r}{\partial z} \tag{4}$$

subject to the boundary conditions

$$\left.\begin{aligned} &u=ax, v=a\left(m-1\right)y, w=-W,\\ &-k_f\frac{\partial T}{\partial z}=h\left(T_f-T\right) at\ z=0\\ &u\to 0, v\to 0, T\to T_\infty\ as\ z\to\infty \end{aligned}\right\} \tag{5}$$

where $a<0$ for shrinking sheet. The sheet shrinks along *x*-direction only when *m* = 1 and that shrinks axi-symmetrically for *m* = 2. The boundary condition (5) signifies that the sheet shrinks with uniform velocities and the sheet involves the constant wall mass transfer velocity. It also signifies that convective heat transfer takes place at the boundary surface. It determines the temperature gradient and heat transfer rate at the boundary surface in the flow system as considered by Hayat et al.[12,18]. Here h is the convective heat transfer coefficient and T_f is the convective fluid temperatue.

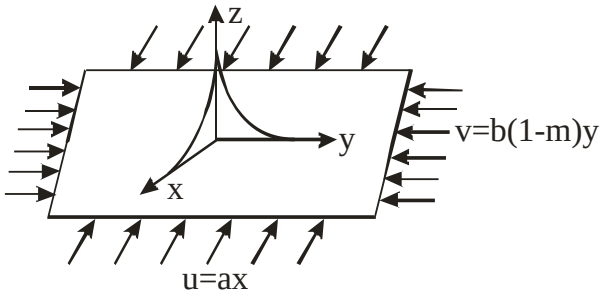

Fig.1 Flow Geometry

The characteristic parameters of the nanofluid [17] are defined as

$$\rho_{nf} = (1-\phi)\,\rho + \phi\rho_s \tag{6}$$

$$\mu_{nf} = \frac{\mu_f}{(1-\phi)^{2.5}} \tag{7}$$

$$\alpha_{nf} = \frac{k_{nf}}{(\rho C_p)_{nf}} \tag{8}$$

$$(\rho C_p)_{nf} = (1-\phi)(\rho C_p)_f + \phi(\rho C_p)_s \tag{9}$$

$$\frac{k_{nf}}{k_f} = \frac{k_s + 2k_f - 2\phi\left(k_f - k_s\right)}{k_s + 2k_f + \phi\left(k_f - k_s\right)} \tag{10}$$

Introducing the variables [12]

$$\left.\begin{aligned} u = cxf'(\eta), v = c(m-1)\,y\,f'(\eta), w = -\sqrt{c\upsilon_f}.m.\,f(\eta) \\ \eta = \sqrt{\frac{c}{\upsilon_f}}\,z, \theta(\eta) = \frac{T-T_\infty}{T_f - T_\infty} \end{aligned}\right\} \tag{11}$$

Equation (1) is satisfied by the velocity components (u, v, w) indicating that the fluid flow is feasible. Here c > 0.

The radiative heat flux using Rosseland approximation [19] is given by

$$q_r = -\frac{4\sigma^*}{3k_1}\frac{\partial T^4}{\partial z} \tag{12}$$

Assume that the differences in temperature within the flow are such that T^4 can be expressed as a linear combination of the temperature. Thus, expanding T^4 in a Taylor series about T_∞ and neglecting higher order terms, we obtain

$$T^4 \approx 4T_\infty^3 T - 3T_\infty^4 \tag{13}$$

Thus, $$\frac{\partial q_r}{\partial z} = \frac{-16\sigma^* T_\infty^3}{3k_1}\frac{\partial^2 T}{\partial z^2} \tag{14}$$

So, eqn. (4) becomes

$$u\frac{\partial T}{\partial x} + v\frac{\partial T}{\partial y} + w\frac{\partial T}{\partial z} = \alpha_{nf}\frac{\partial^2 T}{\partial z^2} + \frac{16\sigma^* T_\infty^3}{3k_1\left(\rho C_p\right)_{nf}}\frac{\partial^2 T}{\partial z^2} \tag{15}$$

Using (6)-(11), eqns. (2), (3) and (15) take the form

$$f''' + (1-\phi)^{2.5}\left[1-\phi+\left(\frac{\rho_s}{\rho_f}\right)\phi\right]\left\{mff'' - (f')^2\right\} - (1-\phi)^{2.5}.A.M.f' - A.K_p.f' = 0 \tag{16}$$

$$\frac{1}{P_r}\left(\frac{k_{nf}}{k_f} + R\right)\theta'' + \left[1-\phi+\left\{\frac{\left(\rho c_p\right)_s}{\left(\rho c_p\right)_f}\right\}\phi\right]mf\theta' = 0 \tag{17}$$

where

$$\left.\begin{aligned} M &= \frac{\sigma B_0^2}{c\rho_f}, K_p = \frac{\upsilon_f}{cK_p^*}, R = \frac{16\sigma^* T_\infty^3}{3kk_1}, \\ P_r &= \frac{\upsilon_f\left(\rho C_p\right)_f}{k_f}, A = \frac{a}{c} \end{aligned}\right\} \tag{18}$$

with appropriate boundary conditions

$$\left.\begin{aligned} &f = f_w, f' = A, \theta' = -B_i(1-\theta) \text{ at } \eta = 0 \\ &f' \to 0, \theta \to 0 \text{ as } \eta \to \infty \end{aligned}\right\} \tag{19}$$

where $f_w = \dfrac{W}{m\left(\sqrt{c\upsilon_f}\right)}$ is the wall mass transfer parameter with $f_w > 0$ indicates mass suction and

$f_w < 0$ indicates mass injection, $A = \dfrac{a}{c}$ *and* $B_i = \dfrac{h}{k_f}.\sqrt{\dfrac{\upsilon_f}{c}}$.

The skin friction coefficient C_f and local Nusselt number Nu_x are determined respectively as

$$C_f = \frac{\tau_w}{\rho_f u_w^2} \quad \text{and} \quad N_{u_x} = \frac{q_w}{k_f\left(T_f - T_\infty\right)} \tag{20}$$

where $\tau_w = \mu_{nf}\left(\frac{\partial u}{\partial z}\right)_{z=0}$ represents the wall shear stress at the shrinking surface and $q_w = -k_{nf}\left(\frac{\partial T}{\partial z}\right)_{z=0}$ represents the wall heat flux from the shrinking surface.

The dimensionless form of skin-friction coefficient and local Nusselt number can be obtained respectively as

$$Re_x^{1/2} C_f = \frac{f''(0)}{(1-\phi)^{2.5}} \text{ and } Re_x^{-1/2} Nu_x = \frac{-k_{nf}}{k_f}\theta'(0) \tag{21}$$

3. Homotopy solutions

Let us choose the initial approximations and auxiliary linear operators for homotopy analysis solutions as

$$f_0(\eta) = f_w + A\left[1 - e^{-n}\right], \theta_0(\eta) = \frac{B_i}{1+B_i} e^{-\eta} \tag{22}$$

$$L(f) = f''' - f', L(\theta) = \theta'' - \theta \tag{23}$$

The above auxiliary linear operators satisfy the following properties:

$$\left.\begin{aligned} L(f)\left[c_1 + c_2 e^{\eta} + c_3 e^{-\eta}\right] = 0 \\ L(\theta)\left[c_4 e^{\eta} + c_5 e^{-\eta}\right] = 0 \end{aligned}\right\} \tag{24}$$

including c_1 to c_5 as arbitrary constants.

Following Liao [20], Abbasbandy and Shirzadi [21], the associated zeroth order deformation problems can be obtained as:

$$(1-p)(f)\left[\hat{f}(\eta, p) - f_0(\eta)\right] = p\hbar_f N_f\left[\hat{f}(\eta, p)\right] \tag{25}$$

$$(1-p)(\theta)\left[\hat{\theta}(\eta, p) - \theta_0(\eta)\right] = p\hbar_\theta N_\theta\left[\hat{\theta}(\eta, p)\right] \tag{26}$$

$$\left.\begin{aligned}\hat{f}(0,p)=f_w,\hat{f}'(0,p)=A,\hat{f}'(\infty,p)=0\\ \hat{\theta}'(0,p)=-B_i\left[1-\theta(0,p)\right],\hat{\theta}(\infty,p)=0\end{aligned}\right\} \tag{27}$$

where p represents an embedding parameter, $\hbar_f$ and $\hbar_\theta$ are non-zero auxiliary parameters.

The non-linear operators N_f and N_θ are respectively

$$N_f\left[\hat{f}(\eta,p),\hat{\theta}(\eta,p)\right]=\frac{\partial^3\hat{f}(\eta,p)}{\partial\eta^3}+(1-\phi)^{2.5}\left[1-\phi+\left(\frac{\rho_s}{\rho_f}\right)\phi\right]$$

$$\times\left\{m.\hat{f}(\eta,p).\frac{\partial^2\hat{f}(\eta,p)}{\partial\eta^2}-\left[\frac{\partial\hat{f}(\eta,p)}{\partial\eta}\right]^2\right\}$$

$$-(1-\phi)^{2.5}.A.M\frac{\partial\hat{f}(\eta,p)}{\partial\eta}-A.K_p\frac{\partial\hat{f}(\eta,p)}{\partial\eta} \tag{28}$$

$$N_\theta\left[\hat{\theta}(\eta,p),\hat{f}(\eta,p)\right]=\frac{1}{P_r}\left(\frac{k_{nf}}{k_f}+R\right)\frac{\partial^2\hat{\theta}(\eta,p)}{\partial\eta^2}+\left[1-\phi+\left\{\frac{(\rho c_p)_s}{(\rho c_p)_f}\right\}\phi\right]m\hat{f}(\eta,p)\frac{\partial\hat{\theta}(\eta,p)}{\partial\eta} \tag{29}$$

When $p=0$ and $p=1$, we obtain

$$\hat{f}(\eta,0)=f_0(\eta),\hat{\theta}(\eta,0)=\theta_0(\eta),\ \hat{f}(\eta,1)=f(\eta)\text{ and }\hat{\theta}(\eta,1)=\theta(\eta) \tag{30}$$

When p increases from 0 to 1, $f(\eta,p)$ varies from $f_0(\eta)$ to $f(\eta)$ and $\theta(\eta,p)$ varies from $\theta_0(\eta)$ to $\theta(\eta)$.

With the help of Taylor's expansion, we can obtain

$$f(\eta,p)=f_0(\eta)+\sum_{n=1}^{\infty}f_n(\eta)\,p^n,f_n(\eta)=\frac{1}{n!}\frac{\partial^n f(\eta,p)}{\partial\eta^n}\bigg|_{p=0} \tag{31}$$

$$\theta(\eta,p)=\theta_0(\eta)+\sum_{n=1}^{\infty}\theta_n(\eta)\,p^n,\theta_n(\eta)=\frac{1}{n!}\frac{\partial^n\theta(\eta,p)}{\partial\eta^n}\bigg|_{p=0} \tag{32}$$

The convergence of the above series depends upon $\hbar_f$ and $\hbar_\theta$. Assume that $\hbar_f$ and $\hbar_\theta$ are properly chosen so that eqns. (31) and (32) converge at $p=1$. So we have

$$f(\eta)=f_0(\eta)+\sum_{n=1}^{\infty}f_n(\eta) \tag{33}$$

$$\theta(\eta) = \theta_0(\eta) + \sum_{n=1}^{\infty} \theta_n(\eta) \tag{34}$$

The general solutions can be obtained as

$$f_n(\eta) = f_n^*(\eta) + c_1 + c_2 e^{\eta} + c_3 e^{-\eta} \tag{35}$$

$$\theta_n(\eta) = \theta_n^*(\eta) + c_4 e^{\eta} + c_5 e^{-\eta} \tag{36}$$

where f_n^* and θ_n^* are special functions.

In this case the values of the constants c_1 to c_5 with the help of boundary conditions

$$f_n(0) = f_n'(0) = f_n'(\infty) = \theta_n'(0) - B_i \theta_n(0) = \theta_n(\infty) = 0 \tag{37}$$

can be obtained as

$$\left.\begin{aligned} c_1 &= -c_3 - f_n^*(0), \\ c_2 &= c_4 = 0, \\ c_3 &= \left.\frac{\partial f_n^*(\eta)}{\partial \eta}\right|_{\eta=0} \\ c_5 &= \frac{1}{1+B_i}\left[\left.\frac{\partial \theta_n^*(\eta)}{\partial \eta}\right|_{\eta=0} - B_i \theta_n^*(0)\right] \end{aligned}\right\} \tag{38}$$

4. Convergence analysis and discussion

The non-dimensional governing equations (16) and (17) of the flow problem have been solved by using Homotopy Analysis Method (HAM). The comprehensive discussion and diagrammatical representation of the influence of various pertinent physical parameters on velocity as well as temperature profiles have been incorporated in the present study.

The HAM solutions involve the auxiliary parameters $\hbar_f$ and $\hbar_\theta$. Hence the $\hbar$- curves for the 14th order approximations have been portrayed to obtain the range for admissible values of $\hbar_f$ and $\hbar_\theta$ for the functions $f''(0)$ and $\theta'(0)$ respectively. According to Figs. 2 and 3, the range of the admissible values of $\hbar_f$ and $\hbar_\theta$ are $-1 \le \hbar_f \le -0.4$ and $-1 \le \hbar_\theta \le -0.2$ respectively. Hence the series solution converge in the whole region of $\eta\ (0 < \eta < \infty)$ when $\hbar_f = -0.5$ and $\hbar_\theta = -0.6$.

Figs. 4-8 reveal the influence of the parameters M, A, K_p, ϕ and f_w on velocity profiles of nanofluid past a shrinking surface. Let us now discuss the influence of these parameters in somewhat detail, one by one. Fig. 4 is well designed to explore and reinvigorate the influence of M on fluid motion. If we enhance M somewhat, then the fluid motion gets retarded. In other words, if there were no applied magnetic field there would no electromagnetic interaction between electrical conducting fluid and the magnetic field and hence retardation of velocity would not be seen. This is in agreement with the results of Hayat et al. [12]. Fig. 5 displays, in rich detail, the fact that increasing A slows down the fluid motion but the magnitude of deceleration is significant. Because of resistive force offered by the porous medium, the velocity profiles get reduced and then the momentum boundary layer shrinks as is plotted in Fig. 5. By looking at Fig. 7, we can say that the fluid motion is enhanced by increasing volume fraction parameter ϕ. Fig. 8 shows the portrayal of velocity distribution of nanofluid for suction $(f_w > 0)$, injection $(f_w < 0)$ and impermeable surface $(f_w = 0)$ in presence of porous matrix. In compliance with the findings of [12], the suction at the surface retards the velocity while the effect of injection is diametrical opposite to that of suction. Here is an interesting consequence of the combined effect of suction and porous matrix favorable to diminution of momentum boundary layer which in turn favors the stability of the flow.

Figs. 9-15 portray the temperature distribution inspired by M, K_p, f_w, R, A, B_i and ϕ respectively. In fact, had there been no M and K_p, the temperature distribution could not be enhanced in the flow field. This means that temperature rising would not be possible without M and K_p. Higher M and K_p enable the temperature to rise. In other words, higher values of M and K_p are responsible for the enhancement of temperature distribution as are sketched in Figs. 9 and 10. This result is in conformity with the result reported earlier by Hayat et al. [12]. Hence thermal boundary layer is an increasing function of M and K_p each. Temperature decreases due to increase in suction parameter, f_w and as a result of it a thinner thermal boundary layer has been accomplished (Fig. 11). Fig.12 depicts that increasing values of radiation parameter R increase the fluid temperature throughout the flow domain developing the wider thermal boundary layer. It is for this reason that thermal radiation plays an important role in regulating temperature of a system and controlling the thermal boundary layers effectively. So, the thermal

radiation parameter should be kept minimum to achieve a better cooling process. This is in agreement with the result claimed by Nandy and Pop [22].

Fig. 1 32 focuses on the characteristics of fluid temperature inspired by *A.* It is noticed that increasing *A* decreases the fluid temperature in presence of thermal radiation. Fig. 14 describes that enhancement of B_i increases the temperature, however this effect is more pronounced in the region contiguous to the solid surface. The early indications in Fig. 15 are the behavior of temperature under the influence of volume fraction parameter ϕ where the temperature increases with increase in ϕ in the entire flow domain. Therefore, the thickness of the temperature boundary layer gets enhanced.

Table – 1 Thermo physical properties of water and nanoparticles.

	$\rho(kg.m^{-3})$	$C_p(J.kg^{-1}.k^{-1})$	$k(W.m^{-1}k^{-1})$	$\beta\times10^5(k^{-1})$
Pure water (H_2O)	997.1	4179	0.613	21
Copper (Cu)	8933	385	40	1.67
Silver (Ag)	10500	235	429	1.89
Alumina (Al_2O_3)	3970	765	40	0.85
Titanium oxide (TiO_2)	4250	686.2	8.9538	0.9

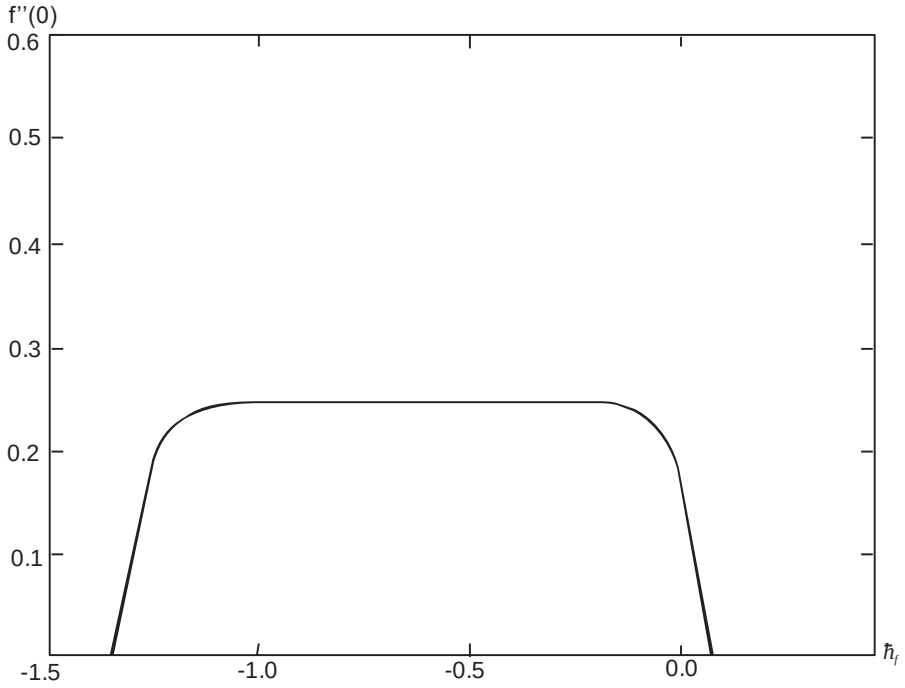

Fig. 2 $\hbar-$ **curve for *f* in Cu-water nanofluid with**

$M=0.2,\ f_w=0.5, m=2, A=-0.1, \phi=B_i=0.1, K_p=0.5$ **.**

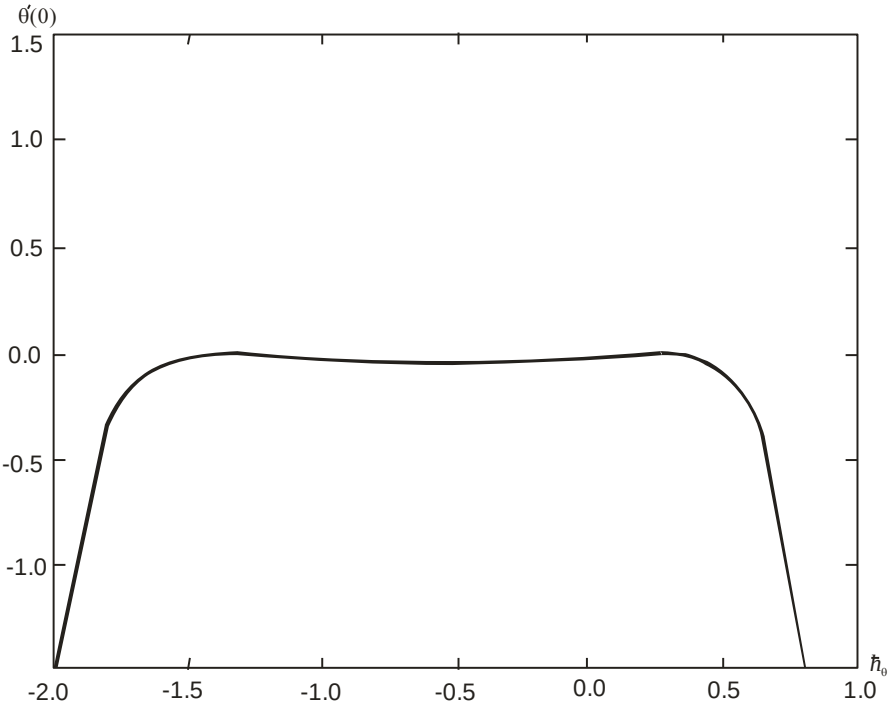

Fig. 3 $\hbar-$ **curve for** θ **in Cu-water nanofluid with**

$M=0.2,\ f_w=0.5, m=2, A=-0.1, \phi=B_i=0.1, K_p=0.5, P_r=6.2, R=0.5$ **.**

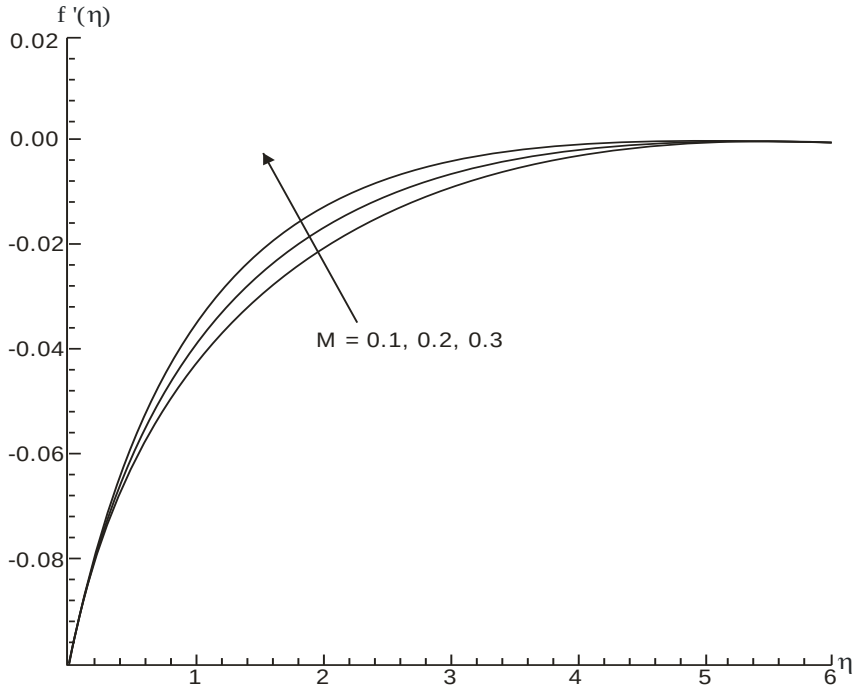

Fig. 4 Influence of M on velocity for $f_w = 0.5, m = 2, A = -0.1, \phi = 0.1, K_p = 0.5$.

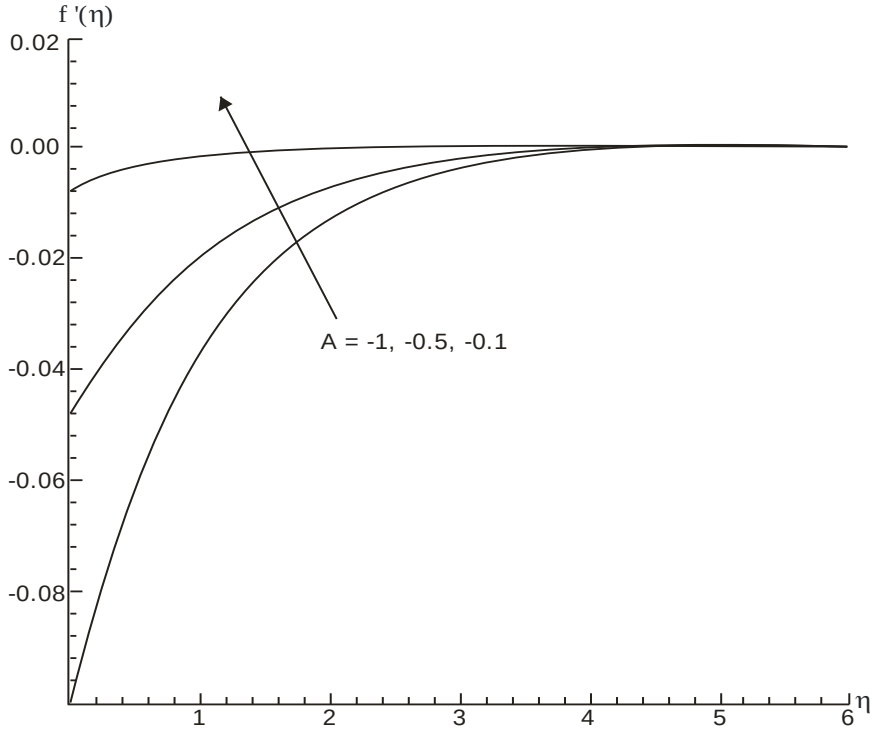

Fig. 5 Influence of A on velocity for $f_w = 0.5, m = 2, M = 0.2, \phi = 0.1, K_p = 0.5$.

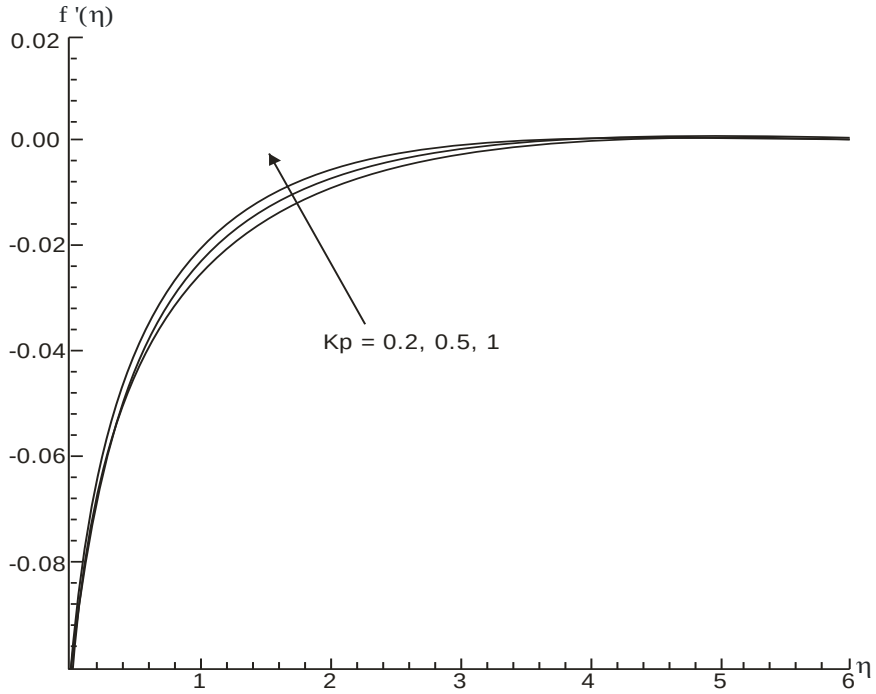

Fig. 6 Influence of K_p on velocity for $f_w = 0.5, m = 2, M = 0.2, \phi = 0.1, A = -0.1.$

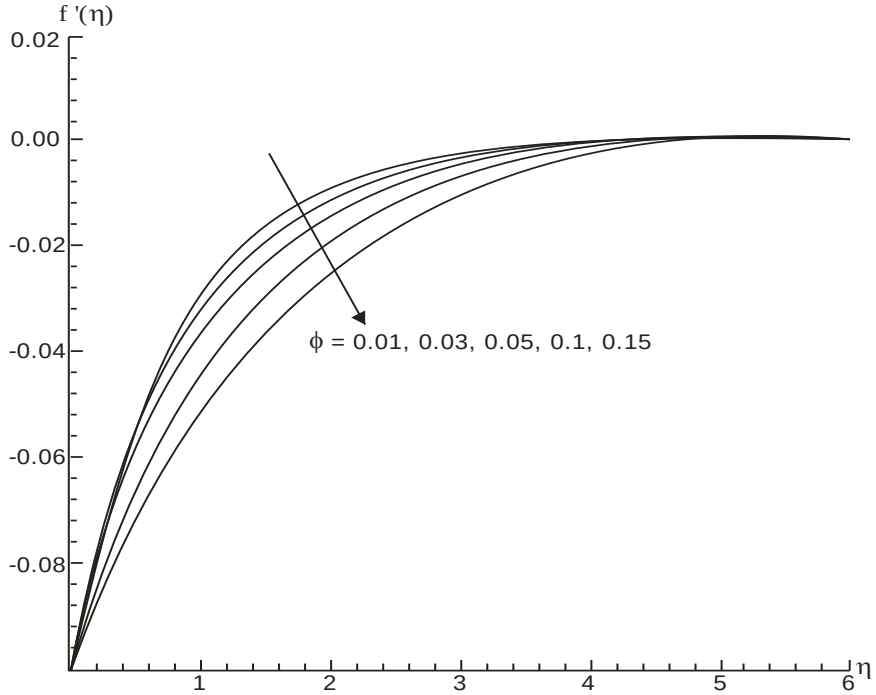

Fig. 7 Influence of ϕ on velocity for $f_w = 0.5, m = 2, M = 0.2, K_p = 0.5, A = -0.1.$

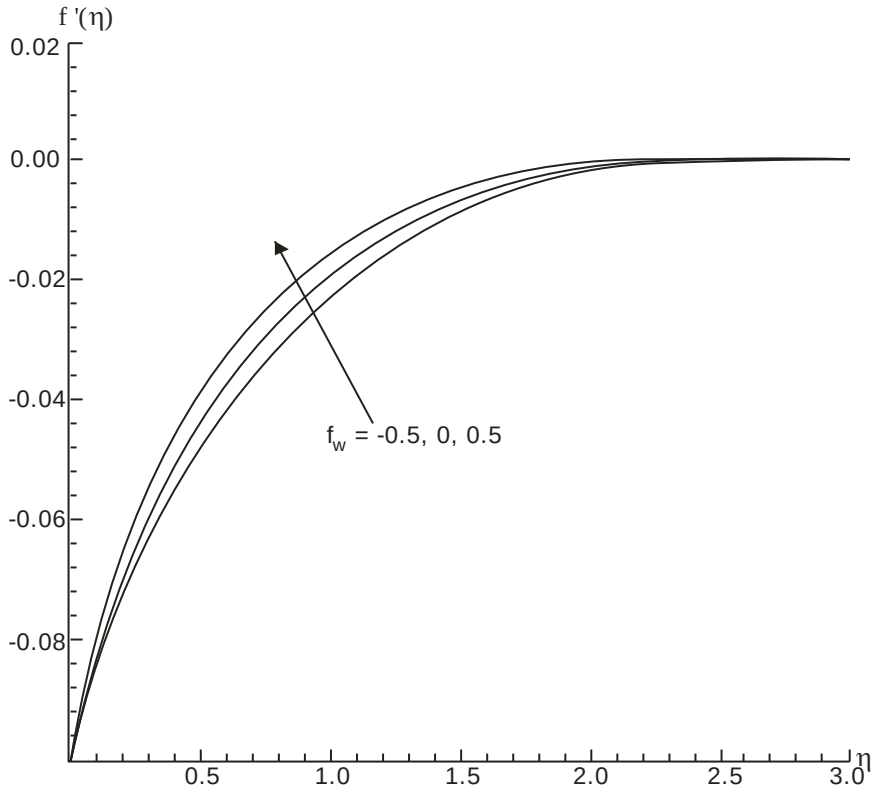

Fig. 8 Influence of f_w on velocity for $\phi = 0.1, m = 2, M = 0.2, K_p = 0.5, A = -0.1.$

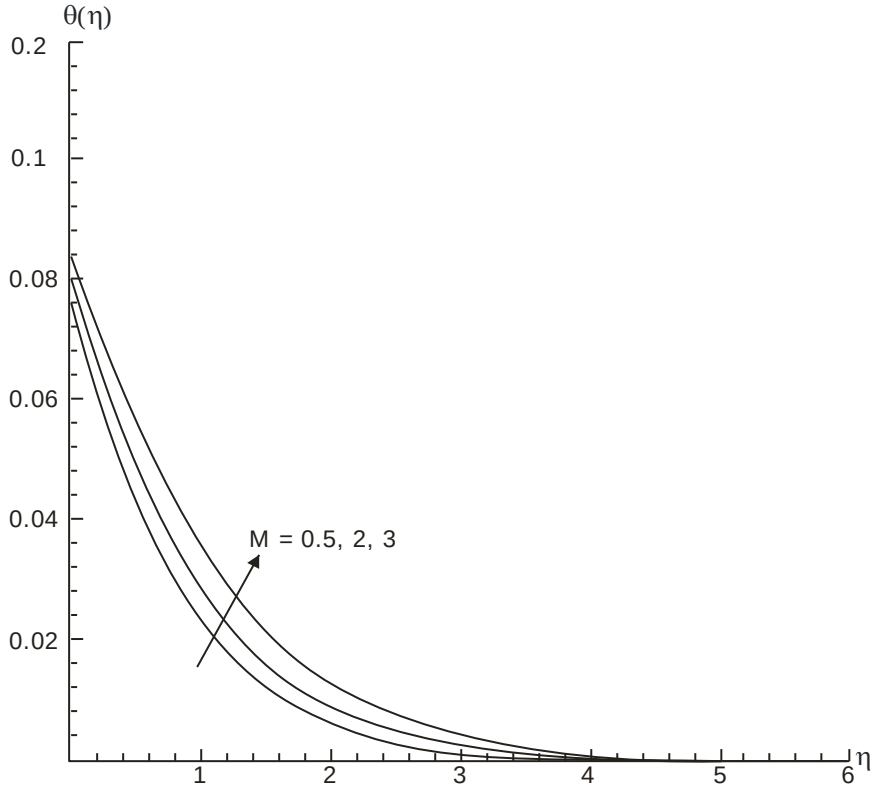

Fig. 9 Influence of M on temperature for
$K_p = 0.5,\ f_w = 0.5, A = -0.1, m = 2, R = 0.5, \phi = B_i = 0.1, P_r = 6.2$.

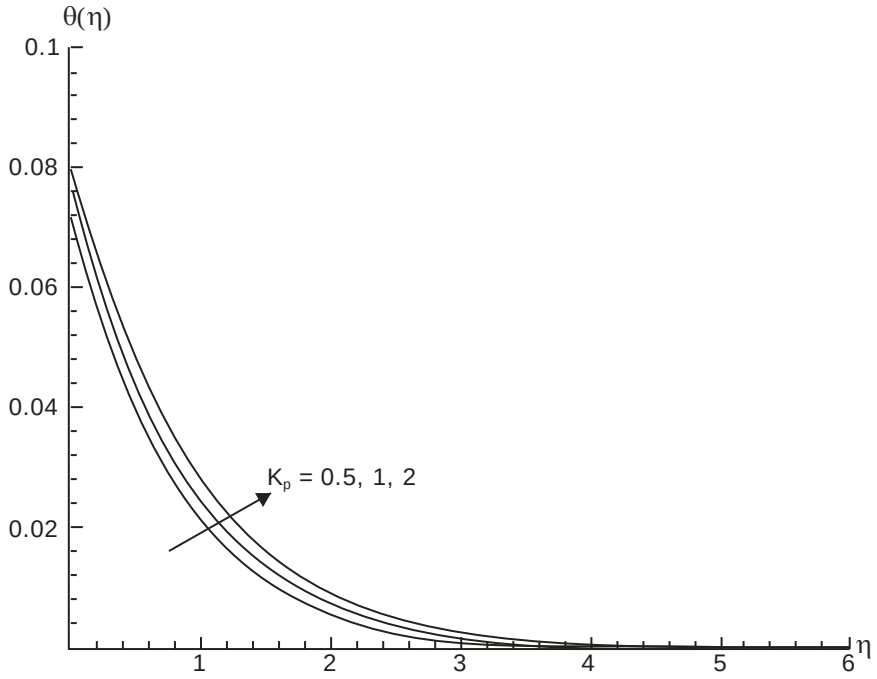

Fig. 10 Influence of K_p on temperature for

$M = 0.2,\ f_w = 0.5, A = -0.1, m = 2, R = 0.5 \phi = B_i = 0.1, P_r = 6.2$.

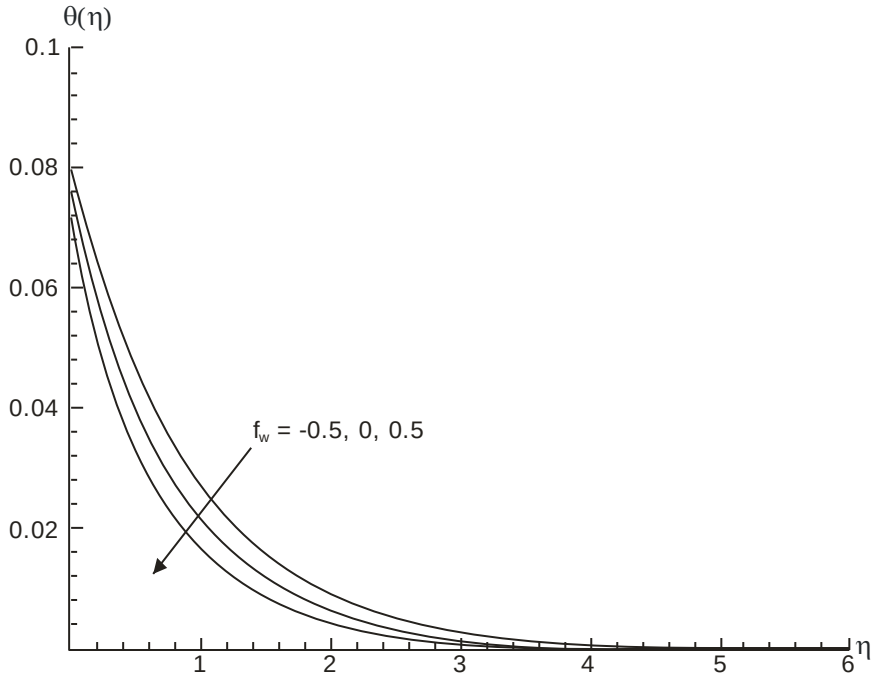

Fig. 11 Influence of f_w on temperature for

$M = 0.2, K_p = 0.5, A = -0.1, m = 2, R = 0.5 \phi = B_i = 0.1, P_r = 6.2$.

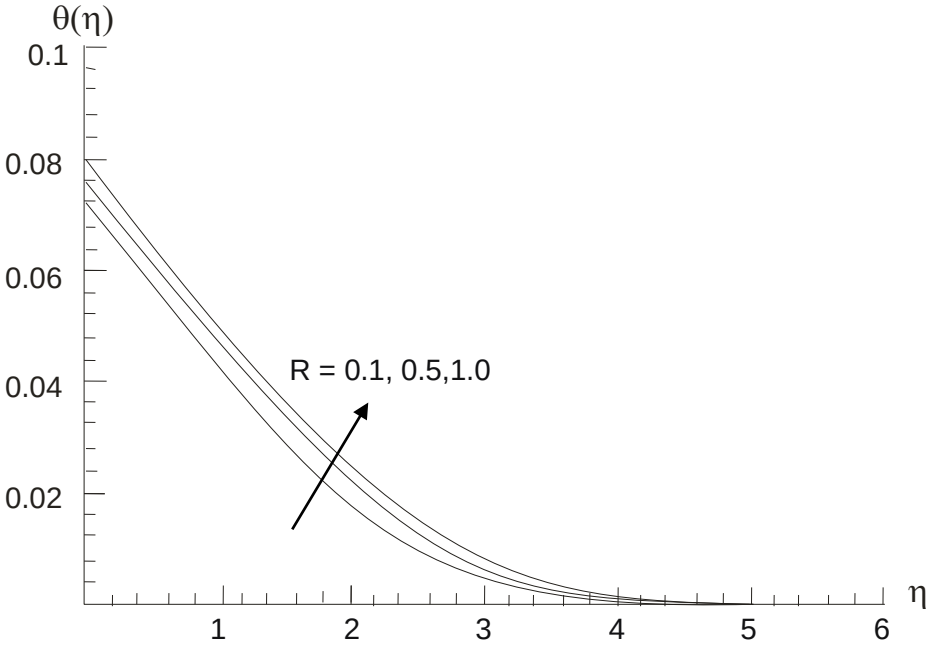

Fig. 12 Influence of R on temperature for
$M = 0.2, K_p = 0.5, A = -0.1, m = 2,\ f_w = 0.5,\ \phi = B_i = 0.1, P_r = 6.2$.

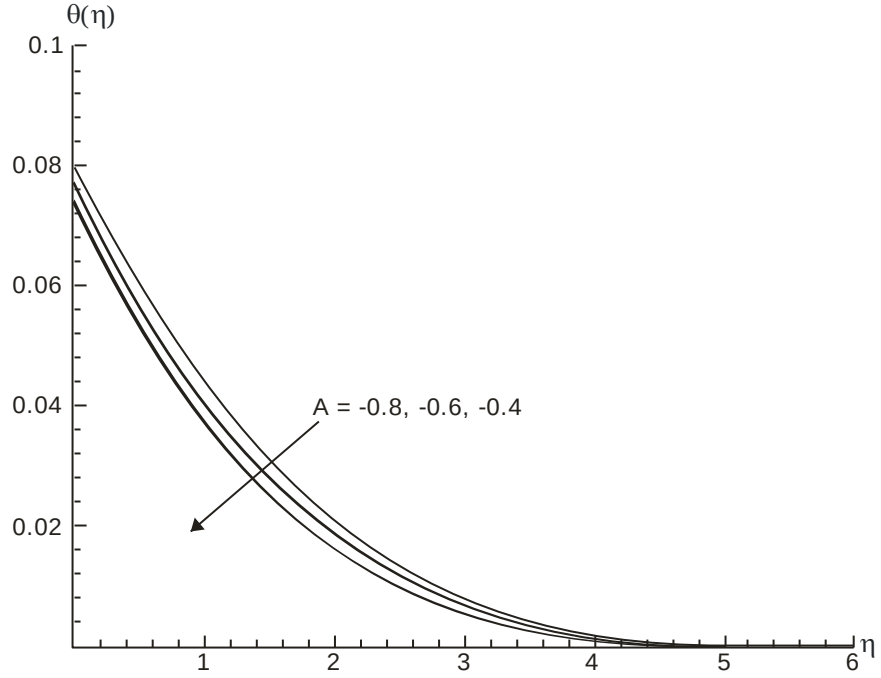

Fig. 13 Influence of A on temperature for
$M = 0.2, K_p = 0.5 m = 2,\ f_w = 0.5, R = 0.2, \phi = B_i = 0.1, P_r = 6.2$.

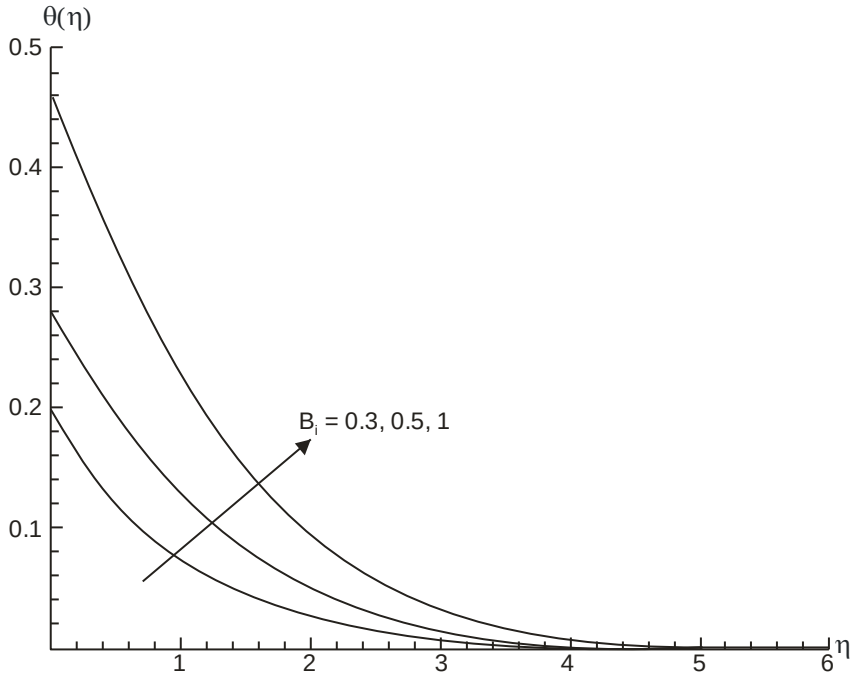

Fig. 14 Influence of B_i on temperature for

$M = 0.2, K_p = 0.5, m = 2,\ f_w = 0.5, A = -0.1, R = 0.2, \phi = 0.1, P_r = 6.2$.

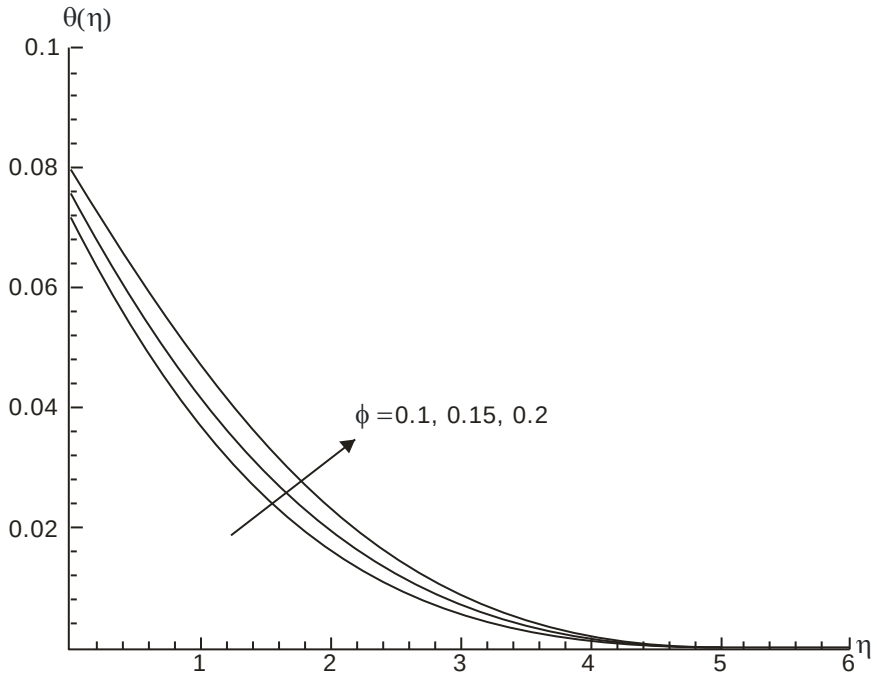

Fig. 15 Influence of ϕ on temperature for

$M = 0.2, K_p = 0.5, m = 2,\ f_w = 0.5, A = -0.1, R = 0.2, B_i = 0.1, P_r = 6.2$.

5. Conclusion

In the present study, the effect of thermal radiation for MHD 3D flow of nanofluid past a shrinking surface has been thoroughly discussed and presented graphically. The specific conclusions derived from this study can be summarized as follows:

The presence of the magnetic field and porous matrix thins hydrodynamic boundary layer and develops a thicker temperature boundary layer. Temperature in thermal boundary layer falls due to increase in the value of *R* and as a consequence the associated thermal boundary layer becomes thinner and thinner. Increase in the values of wall mass transfer parameter f_w diminishes the velocity as well as the temperature profiles and thereby the momentum and thermal boundary layer shrink. The behavior of A is diametrically opposite to that of ϕ temperature distribution.

References

[1] E.G. Fischer, Extrusion of plastics, New York: Wiley, 1976.

[2] T. Altan, Metal forming fundamentals and applications, Metals Park (OH): American Society of Metals, 1979.

[3] B.C. Sakiadis, Boundary layer behavior on continuous solid surfaces, AICHE J. 7 (1961) 26-28.

[4] F.K. Tsou, E.M. Sparrow, R. J. Golstain, Flow and heat transfer in the boundary-layer on a continuous moving surface, Int. J. Heat Mass Transfer, 10 (1967) 219-235.

[5] M. K. Nayak, Chemical reaction effect on MHD viscoelastic fluid over a stretching sheet through porous medium, Meccanica, DOI 10.1007/s11012-015-0329-3.

[6] A. Raptis, C. Perdikis, Viscous flow over a non-linearly stretching sheet in the presence of a chemical reaction and magnetic field, Int. J. Non-Linear Mech. 41 (2006) 527–529.

[7] J.C. Arnold, A.A. Asir, S. Somasundaram, T. Christopher, Heat transfer in a viscoelastic boundary layer flow over a stretching sheet, Int. J. Heat Mass Transfer 53 (2010) 1112–8.

[8] C-H Chen, Combined effects of joule heating and viscous dissipation on magnetohydrodynamic flow past a permeable stretching surface with free convection and radiative heat transfer, J. Heat Transfer 132 (2010) 064503.

[9] S. U. S. Choi, Enhancing thermal conductivity of fluids with nanoparticles, ASME Fluids Eng. Division, 231 (1995) 99–105.

[10] Y. Xuan, Q. Li, Investigation on convective heat transfer and flow features of nanofluids, J. Heat Transfer, 125 (2003) 151-155.

[11] M. K. Nayak, Nanoscience and Technology, 2ed., India Tech, New Delhi, 2015.

[12] T. Hayat, M. Imtiaz, A. Alsaedi, MHD 3D flow of nanofluid in presence of convective conditions, J. Mol. Liq. 212 (2015) 203-208.

[13] N. S. Akber, S. Nadeem, R. Ul Haq, Z. H. khan, Radiation effects on MHD stagnation point flow of nanofluid towards a stretching surface with convective boundary condition, Chin. J. Aeronaut. 26 (6) (2013) 1389-1397.

[14] M. K. Nayak, G. C. Dash, L. P. Singh, Unsteady radiative MHD free convective flow and mass transfer of a viscoelastic fluid past an inclined porous plate, Arab. J. Sci. Eng., 40 (2015) 3029-3039.

[15] M. Wahiduzzamana, Md. S. Khanb, I. Karim , MHD Convective Stagnation Flow of Nanofluid over a Shrinking Surface with Thermal Radiation, Heat Generation and Chemical Reaction, Procedia Eng. 105 (2015) 398–405.

[16] M. K. Nayak, G.C. Dash, L.P. Singh**,** Flow and mass transfer analysis of a micropolar fluid in a vertical channel with heat source and chemical reaction, AMSE Journals, Series: Modelling B, 84 (1) (2015) 69-91.

[17] A. Mahdy, Unsteady mixed convection boundary layer flow and heat transfer of nanofluids due to stretching sheet, Nuclear Engineering and Design 249 (2012) 248-255.

[18] T. Hayat, T. Muhammad, S.A. Sehezad, G. Q. Chen, I. A. Abbas, Interaction of magnetic field in flow of Maxwell nanofluid with convective effect, J. Magn. Magn. Mater. 389 (2015) 48-55.

[19] M. Q. Brewster, Thermal radiative transfer properties, Wiley, New York, (1972).

[20] S. J. Liao, Beyond Perturbation: Introduction to Homotopy Analysis Method. Chapman and Hall, CRC Press, Boca Raton, 2003.

[21] S. Abbasbandy, A. Shirzadi, A new application of the homotopy analysis method: solving the Strum–Liouville problems. Commun. Nonlinear Sci. Numer. Simul. 16 (2011) 112–126.

[22] D. Pal, G. Mandal, K. Vajravelu, Flow and heat transfer of nanofluids at a stagnation point flow over a stretching/shrinking surface in a porous medium with thermal radiation, Appl. Math. Comput. 238 (2014) 208-224.